1970

Strength of wide-flange sections under combined axial force and weak-axis bending, October 1970.

John M. Lybas

Wide-Flange Beam-Columns Bent About Weak-Axis

STRENGTH OF WIDE-FLANGE SECTIONS UNDER COMBINED AXIAL FORCE AND WEAK-AXIS BENDING

by

John M. Lybas

This work has been carried out as part of an investigation sponsored by the American Institute of Steel Construction.

Fritz Engineering Laboratory
Lehigh University
Bethlehem, Pennsylvania

October 1970

Fritz Engineering Laboratory Report No. 361.1

TABLE OF CONTENTS

ABSTRACT

The results of two eccentrically loaded stub column tests are presented in this report. In the tests, the columns were oriented in such a way that the applied load causes bending about the weak axis of the cross section. The tests were performed to study the plastic strength of wide-flange bending, with particular emphasis on flange local buckling and deformation capacity in the inelastic range. The results obtained indicate that the load-carrying capacity of these sections can be predicted accurately by the plastic theory and that the limiting flange width-to-thickness ratio developed previously for strong axis bending is conservative when used in weak-axis bending.

1. INTRODUCTION

In a rigidly jointed multi-story frame, the columns are usually subjected to combined axial force and bending moment. When the axial force is relatively high, it is sometimes advantageous to orient the columns in such a way that the applied moment will cause bending about their weak axis.[1] This is done to avoid lateral-torsional buckling which is often associated with strong axis bending.[2,3] Also, when two-way rigid framing systems are used for a building, the columns will be subjected to a certain amount of weak axis bending. In this case, of course, both strong axis and weak axis bending effects will be present.

The work reported in this paper is an exploratory study on the strength of wide-flange sections under combined axial force and weak-axis bending, with particular emphasis on the deformation capacity in the inelastic range. The information is of basic importance in the study of beam-columns subjected to weak-axis bending. In order to explain fully the objectives of this research, it is necessary to review briefly the general behavior of beam-columns. Figure 1 shows a beam-column subjected to a constant axial force P, and end moments, M_o causing double (or reversed) curvature deformation. At any section along the length of this member, the bending moment is equal to sum of the moment due to M_o (linearly varying), and the secondary moment, $P\delta$, induced by the deflection δ at the section. The variation of the total moment is as shown in Fig. 2. For a relatively short column, the largest moment will occur at the ends.[4] (See Fig. 2a). Therefore,

yielding will take place first at the two ends, and eventually plastic hinges will develop at these locations. The general behavior of this column is illustrated in Fig. 3a which gives the relationship between the applied moment, M_o, and the resulting rotation θ. At first the rotation increases linearly with the moment. When yielding first occurs in the material, the relationship becomes non-linear, but the rotation continues to increase with the applied moment. Eventually, a maximum moment, which is equal to the plastic moment (reduced for the effect of axial force) of the section, will be reached. The column will be "free" to rotate under this maximum moment. The ability to rotate without unloading is an important requirement in plastic design. If the column is sufficiently long, the largest moment will occur at an interior section (see Fig. 2b). In this case, the effect of column instability due to the $P\delta$ moment will significantly change the behavior of the member after the maximum moment is reached. In order to maintain equilibrium at the critical section, the applied moment must be reduced as soon as its maximum value is attained.* The moment-rotation relationship for this case is shown in Fig. 3b.

The general behavior illustrated in Figs. 3a and 3b will be significantly altered if the compression flange (or the web) of the critical section (where the largest moment occurs) starts to buckle like a plate element. This type of buckling is often referred to as "local buckling". The dashed lines in Figs. 3a and 3b depict the possible influence of local buckling. In general, the strength or the deformation capacity will be reduced by local buckling. The controlling parameter

---

*For a more detailed discussion on the instability effect in beam-columns, see Ref. 5.

for flange buckling is the width-to-thickness, b/t, ratio. Up to now, it has not been possible to find a limiting b/t ratio suitable for wide-flange sections under weak-axis bending. For this reason, the present AISC Specification requires that for weak-axis bending the sections should meet the same b/t limitation as for strong-axis bending. This, of course, is likely to be very conservative, because in the case of strong-axis bending the compression flange is under uniform stress, while for weak-axis bending, there will be a stress gradient across the flange. For A36 steel, the limiting b/t for strong-axis bending is 17 for sections to be used in plastic design.[6]

The following are the objectives of the research described in this paper:

1. To study the strength of wide-flange sections subjected to combined axial force and weak-axis bending.
2. To check by experiments the adequacy of using the limiting b/t ratio developed previously for strong axis bending in the case of weak-axis bending.

These objectives are accomplished by carrying out two eccentrically loaded stub column tests, the details of which will be described in the next section.

2. DESCRIPTION OF TESTS

2.1 Test Specimens

The experimental part of this research consisted of two tests of eccentrically loaded stub columns. In both tests, the specimen was an 8WF35 section, 26 in. in length. These two tests differed only in the eccentricity of the axial load. In the first test, the eccentricity was to be 0.92 in. In the second test the intended eccentricity was 2.77 in. The 8WF35 section was chosen on the basis of two considerations. The first of these was that this section had its flange width and its depth very nearly equal. Hence, it is a section likely to be used as a column. The second consideration was that it had a b/t ratio very close to the limiting ratio (16.3 vs. 17.0). Hence, the 8WF35 section would provide a reasonably good test of the adequacy of the limiting b/t ratio (objective 2 stated in Chapter 1). The length was chosen so as to obtain an undisturbed residual stress pattern over a 10" gage length.

The axial load eccentricities for the test specimens were selected to provide two distinct combinations of axial force and bending moment. The first test was for high axial force and low bending moment, and the second test low axial force and high bending moment. These tests would therefore furnish an experimental verification of the theoretical solution developed previously for the case of combined axial force and weak axis bending.[7] The theoretical solution defining

the interaction relation between axial force and bending moment is given by the following two expressions:

$$\frac{M_{pc}}{M_p} = 1.00 - \frac{A^2}{4dZy} \left(\frac{P}{P_y}\right)^2 \qquad (1)$$

$$\left[0 \leq \frac{P}{P_y} \leq \frac{wd}{A} \right]$$

and

$$\frac{M_{pc}}{M_p} = \left[\frac{4bt}{A} - \left(1 - \frac{P}{P_y}\right)\right] \left[1 - \frac{P}{P_y}\right] \frac{A^2}{8tZ_y} \qquad (2)$$

$$\left[\frac{wd}{A} \leq \frac{P}{P_y} \leq 1.00 \right]$$

The symbols used in the above equations are defined as follows:

M_{pc} = reduced plastic moment in the presence of axial force

M_p = plastic moment for P = 0

P = axial load

P_y = axial yield load = area x yield stress ($A \times \sigma_y$)

b,t,d,w = flange width, flange thickness, depth and web thickness, respectively.

A = cross-sectional area

Z_y = plastic modulus about the weak-axis = $\frac{M_p}{\sigma_y}$

By using these equations the interaction diagram, as shown in Fig. 4, was obtained for 8*W*35 shape. The diagram was then divided into three sectors by a line 30^o from the horizontal axis and a second line 30^o from the first. The eccentricities were chosen to have the points representing the ultimate conditions fall where these lines intersect the interaction curve.

2.2 Test Setup

The entire test setup can be seen in Fig. 5. The axial load was applied by an 800 kip universal testing machine. The load was applied through column test fixtures designed to simulate pinned end conditions. One end fixture was placed axially on the testing machine platen; the other was attached axially to the head of the testing machine. Each fixture consisted of two parts -- an outer portion in contact with the testing machine and an inner portion in contact with the specimen. On the part of the inner portion adjacent to the specimen there were two plates. One plate was immoveably and axially attached to the rest of the fixture. The other plate could be moved laterally with respect to the first plate. The specimen was welded axially to the moveable plate. Eccentric loading was obtained through the positioning of the moveable plate with respect to the fixed plate. The details of the test setup have been described in a previous paper.[8]

2.3 Test Procedure and Instrumentation

As each specimen was loaded, the loads were recorded, strains were measured at certain selected points on the specimen, and rotations and deflections were measured. Also, the buckling deformation of the flanges was measured at several points along the specimen. When the specimens behaved elastically, the tests were conducted on a basis of load increments. At the beginning of a test, readings were taken at 20 kip load increments. The size of the increment was decreased as the knee of the theoretical prediction curve (see Figs. 12 and 13) was approached. As the curve became horizontal, it was necessary to conduct the tests on the basis of deflection increments. These increments

were steadily increased in size as the knee of the curve was passed. As each test progressed, a plot was made of load and mid-height deflection. From this plot, it could be ascertained whether sufficient deformation had occurred. If no unloading due to flange buckling was observed, the test was terminated after sufficient deflection had been attained.

During the test, strains were measured by 16 SR-4 strain gages positioned as shown in Fig. 6. Rotations were measured in two ways. Four mechanical rotation gages were mounted on the specimen itself, as shown in Fig. 7. At low loads, however, these were not sensitive enough to measure the rotations. Hence, two dial gages with a least count of 0.0001" were mounted on magnetic bases attached to the linear plates of the test fixtures as shown in Fig. 7.

Deflections were measured at the mid-height, at the ends of the 10" gage length, and at the ends of the specimen by five 0.001" dial gages as illustrated in Fig. 8. The gages were mounted on pedestals resting on the testing machine platen.

In the first test, flange buckling was measured in terms of the change in the distance from the inside corner of web and flange to the inside of the tip of the diagonally opposite flange. This distance was measured with a specially fitted dial gage. This is illustrated in Fig. 9a. This method was found, however, to be less than desirable in terms of both accuracy and ease of execution. In the second test, flange buckling was measured by dial gages attached to the centerline of the flanges and to fixed external supports (Fig. 9b). The fixed

external supports could not move as the specimen deflected laterally. Hence, the gages attached to these supports had to be continually readjusted in order that they would always bear against the desired points on the flange tips. However, since the dial gages attached to the flange centerline moved with the specimen, no such problem was encountered. Hence, from the experiences of this test, one would recommend that flange buckling be measured by dial gages mounted on rigid fixtures rigidly attached to the centerlines of the flanges of the specimen.

3. THEORETICAL ANALYSIS

The theoretical work connected with the investigation pertains to three relations, the interaction relation, the load-deflection relation and the moment-rotation relation.

As explained previously, one of the objectives of the tests was to provide an experimental confirmation of the interaction relationship expressed by Eqs. 1 and 2. The interaction curve shown in Fig. 4 was used to compute the predicted load for each test. After the tests were completed, it was found that the end moments and the top and bottom of specimens were not actually equal because of the slight difference in eccentricities at the two ends. Consequently, the theoretical predictions were adjusted to include this difference by using an average eccentricity. The variation was found to be similar in both tests.

The load computed from the interaction curve was used as the ultimate load in the predicted load-deflection relations. In both tests, the deflection at the mid-height of the specimen was used in plotting the load-deflection relation.

The slope of the linear portion of the load vs. mid-height deflection relation was determined by using the Moment-Area Theorem. The computation for the deflection is shown in Fig. 10.

$$\delta = \int_0^{L/2} \frac{M_x}{EI} \, dx = \frac{M\left(\frac{L}{2}\right)\left(\frac{L}{4}\right)}{EI} = \frac{ML^2}{8EI} = \frac{PeL^2}{8EI} \qquad (3)$$

or

$$\frac{P}{\delta} = \frac{8EI}{eL^2} \qquad (4)$$

in which e is the eccentricity and L the overall length of the specimen. It was decided in this theoretical analysis to ignore the contribution of deflection to moment, because this contribution was found to be extremely small.

The theoretical moment vs. end rotation relation was obtained by utilizing a series of auxiliary curves developed previously for studying the ultimate strength of beam-columns.[9] The moments and rotations used in this theoretical prediction were those occurring at the top or bottom of the 10" gage length. The auxiliary curves were generated by a computer program which was prepared based on the Column Deflection Curve Method.[10] Each curve gives the relationship between the end moment and the resulting end rotation of a beam-column at a constant axial force P. In the tests, the axial force was not constant but varied continuously during testing. Hence, it required additional effort to obtain the desired curves. Using the program, moment-rotation curves were obtained for several values of selected axial load. For a load for which a curve had been plotted, the average deflection at the ends of the gage length was determined by interpolation of the dial gage readings taken during the test. The initial eccentricity had been accurately determined from the strain gage readings in the elastic range. The total eccentricity was taken as the sum of the initial eccentricity and the average deflection at the ends of the gage length. The moment was found from the chosen load multiplied by the total eccentricity. Using this calculated value of moment, the corresponding value of rotation was found from the moment-rotation curve for the particular load being considered. In this manner, a point was found on each of the several moment-rotation curves, each point corresponding to a certain

load. The several points were then connected to obtain the moment-rotation curve for the test. This procedure is illustrated in Fig. 11.

In analyzing the test results, the effect of the deflection at mid-height upon the effective eccentricity of loading at that level was considered. A maximum eccentricity at the mid-height was first determined. Then, for each test, two maximum loads were determined, one corresponding to the initial eccentricity, and the other to the final or maximum load eccentricity.

The above problem also manifested itself in the interaction diagram. For each test, radial lines corresponding to the initial and final eccentricities were drawn out from the origin. The theoretical ultimate condition for a test is then represented by some point on the interaction curve and between the two radial lines.

4. EXPERIMENTAL BEHAVIOR AND DISCUSSION OF RESULTS

The results to be presented pertain primarily to load-deflection relations for each test, moment-rotation relations for each test, and the interaction relation for the 8W35 section. These relations are shown in Figs. 12, 13 and 14. Attempts will be made to compare the theoretical versions of the above relations with experimental results. Consideration will be given to the occurrence of local buckling and the strains attained in the tests.

4.1 Test No. 1

During Test No. 1 the specimen first reached an apparent maximum load very close to the theoretical ultimate load. However, subsequent deformation produced much higher loads. Each time the specimen was allowed to sit overnight under load, the first deformation increment of the next day produced additional load. The test was terminated at Load No. 52, after a large amount of deformation had been achieved without a decrease in load. The onset of local buckling occurred approximately at Load No. 40, and was quite pronounced when the test was finally terminated.

The load vs. mid-height deflection relation for Test No. 1 is shown in Fig. 13a. The experimental curve first reaches a plateau at a load very close to the theoretical ultimate load corresponding to the initial or minimum eccentricity. However, as mentioned above further increase of the applied load was observed continuously during the subsequent testing. The result was that loads far above the

theoretical ultimate were attained. Large inelastic deflections occurred with no decrease in load. The nature of this hardening effect is not fully understood, and further investigation of this problem is necessary.

The moment vs. end rotation relation is shown in Fig. 13b. The experimental curve corresponds very closely to the theoretical relation until shortly after the two curves reach plateaus at almost identical moments. The hardening effect described above then manifests itself in large increases in moment with increased rotation. The experimental relation attained an upper ultimate and then exhibited a slight decrease in moment before the test was terminated.

The interaction relation is shown in Fig. 12. If the ultimate load and the ultimate moment are both considered to correspond to the first plateaus attained, the experimental ultimate condition corresponds almost exactly to the theoretical interaction curve. The experimental point lies in between the lines corresponding to the initial and final eccentricities, as expected. The ultimate condition could also be considered to correspond to the maximum load and maximum moment attained. In this case the experimental ultimate condition lies considerably outside the theoretical interaction curve.

Figures 15 and 16 give the measured strains across the flanges at the mid-height of the specimen for several selected loads. These strains indicate that significant portions of the flanges had reached strain hardening before local buckling occurred. Toward the end of the test maximum strains on the order of 20 times the yield strain were attained at the flange tips. These results are basically

favorable. They imply that the section would be capable of sustaining large amounts of rotation as a plastic hinge. Local buckling does not appear to interfere significantly with the rotation capacity of the section.

The results presented in Figs. 15 and 16 also show that:

1. Strain distribution across the flange is approximately linear, and
2. The location of neutral axis remain essentially uncharged during the application of the load.

The first observation supports the commonly made assumption that plane sections before bending remain plane after bending.

4.2 Test No. 2

In this test inelastic action commenced at a load far below the theoretical ultimate load. This occurred virtually simultaneously with an early onset of local buckling. Considerably higher loads were obtained with further deformation, however. As in the first test, very large deformations were obtained. The test was terminated when each of three successive deformation increments produced a slight decrease in load. At this time yielding and local buckling were quite general.

The load-deflection relation is shown in Fig. 14a. Initially, the experimental relation reaches a plateau at a load significantly below either theoretical ultimate load. At increase values of deflection, however, the load increases, and the theoretical ultimate load corresponding to the maximum eccentricity is attained. Like the hardening effect observed in Test No. 1, the implications of the low

plateau are not fully understood. However, since the formation of the low plateay occurs at approximately the same time as the early onset of local buckling, it seems possible that these two phenomena are related.

The moment-rotation relation is shown in Fig. 14b. The experimental curve reaches a plateau at a moment far below the theoretical ultimate moment. This too might be associated with the premature onset of local buckling. At larger rotations, however, the theoretical ultimate moment is attained and even exceeded. A decrease in moment is noted at the end of the test, implying impending failure.

The agreement with the prediction based on the interaction relation is quite good (Fig. 12). A point representing the maximum load and maximum moment obtained in the test corresponds precisely with the theoretical relation. It does, however, appear to correspond to an eccentricitiy greater than the maximum mid-height eccentricity of loading in the test. This is related to the fact that the maximum load and the maximum moment do not occur at the same load number.

The strain distributions at the mid-height of the specimen are shown for several loads in Figs. 17 and 18. As in the first test, large inelastic deformations occurred and strains on the order of 29 ϵ_y being present when unloading took place. Again it appears that the strain hardening strain was exceeded.

Buckling deformations of the flanges in the second test are shown in Fig. 19. The deformations depict the movement perpendicular to the plane of bending for certain points along the compression side

of the flanges. The movement is measured at the flange tips, at the mid-height and at the ends of the 10" gage length. Local buckling first became noticeable at about Load No. 8, commencing virtually simultaneously with yielding of the section (see Figs. 14a and 14b). Local buckling was quite pronounced at Load No. 22 and became very severe at Load No. 31 when unloading occurred. As in the first test, it does not appear that the onset of local buckling implied immediate failure of the section. Taken as a whole, the test results again imply that the section possesses sufficient rotation capacity for use in plastic design.

5. CONCLUSIONS

The investigation concerns the behavior of wide flange beam-columns under weak-axis bending. It attempts to provide experimental verification of the theoretical load-deflection relation and theoretical moment-rotation relation for wide-flange shapes in weak-axis bending. It also attempts to determine the applicability to weak-axis bending of the AISC limiting b/t ratio, which was derived for strong-axis bending. The study has attempted to achieve its objectives through comparison of the results of two eccentrically loaded stub column tests with a theoretical interaction relation, theoretical load-deflection and moment-rotation relations. The presence of both local buckling and yielding was also considered.

The conclusions derived from the investigation include:

1. The limiting b/t ratios in the AISC Specifications appear to be quite sufficient. Sufficient rotation for use in plastic design was obtained.

2. Actual beam-column ultimate loads and ultimate moments do seem to correspond reasonably well to the theoretical interaction relation.

3. The correspondence of experimental results to theoretical load-deflection relations and theoretical moment-rotation relations was not sufficiently good, nor even sufficiently consistent between the two tests, for reasonable conclusions concerning these aspects of the investigation to be drawn.

6. ACKNOWLEDGMENTS

The work presented in this report is part of an investigation on "Wide-Flange Beam-Columns Bent About Weak Axis" sponsored by the American Institute of Steel Construction. The investigation is under the direction of Dr. Le-Wu Lu, Professor of Civil Engineering and Director of the Plastic Analysis Division, Fritz Engineering Laboratory. The experiments were planned in the summer of 1968 when the author was a recepient of a grant provided by the National Science Foundation under the Undergraduate Research Participation Program.

The report was typed by Miss Karen Philbin and the drawings were prepared by Mr. John Gera.

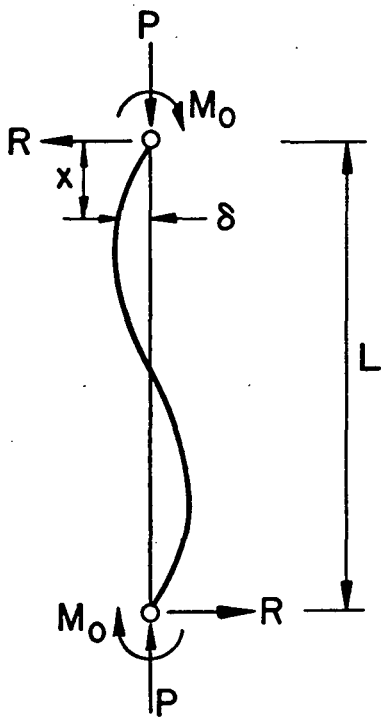

FIG. 1 BEAM-COLUMN UNDER DOUBLE CURVATURE BENDING

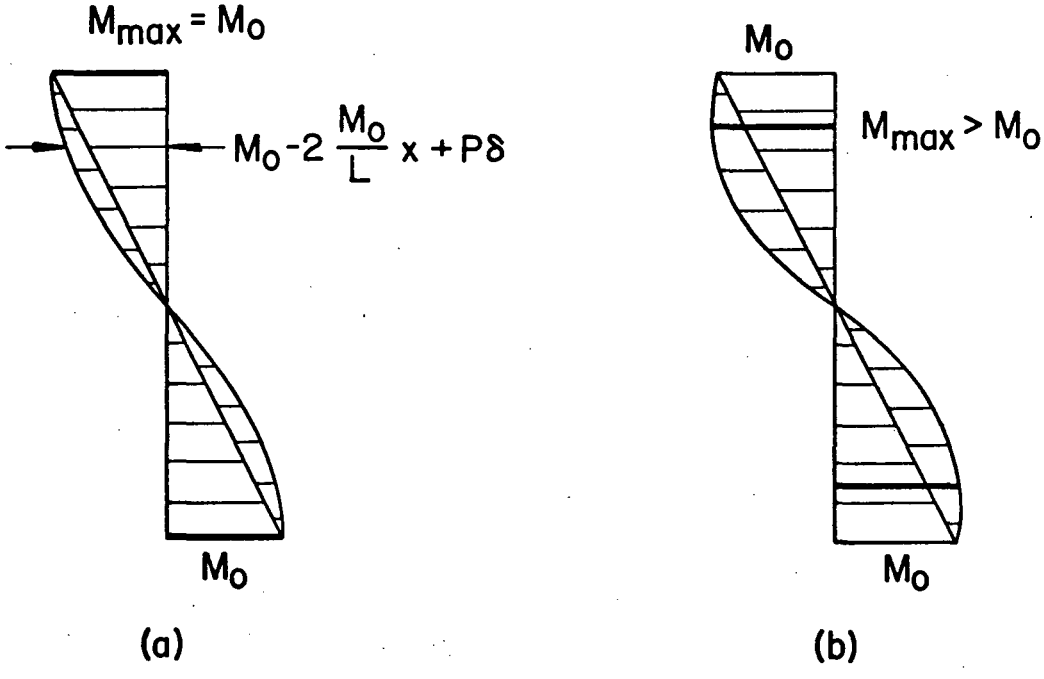

FIG. 2 MOMENT DIAGRAMS FOR BEAM-COLUMNS

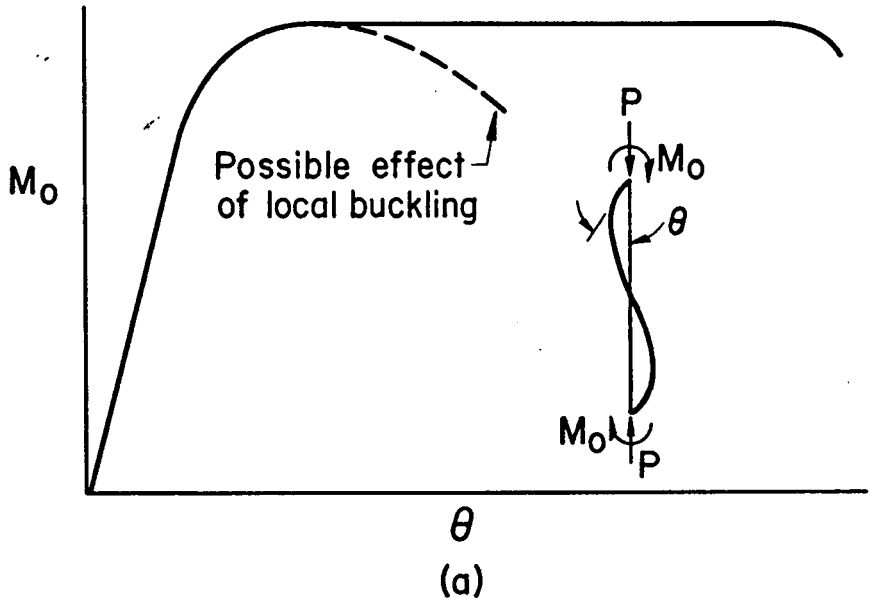

(a)

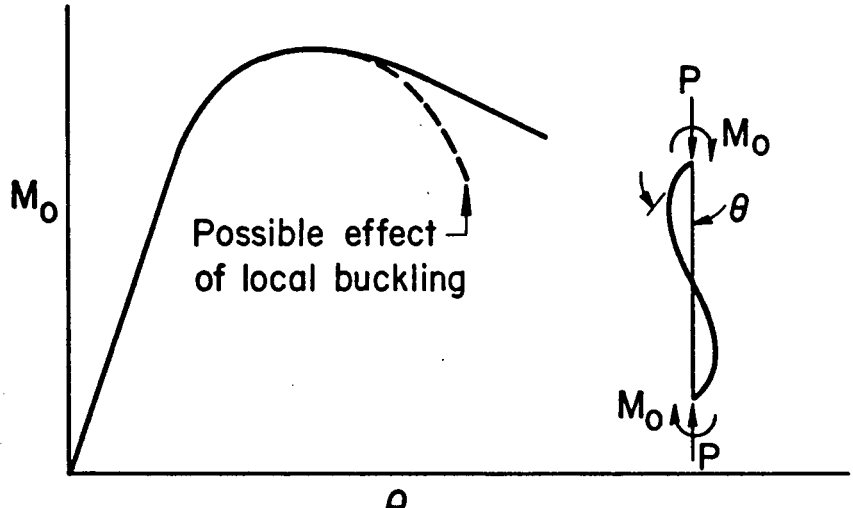

(b)

FIG. 3 MOMENT-ROTATION RELATIONSHIPS OF BEAM-COLUMNS

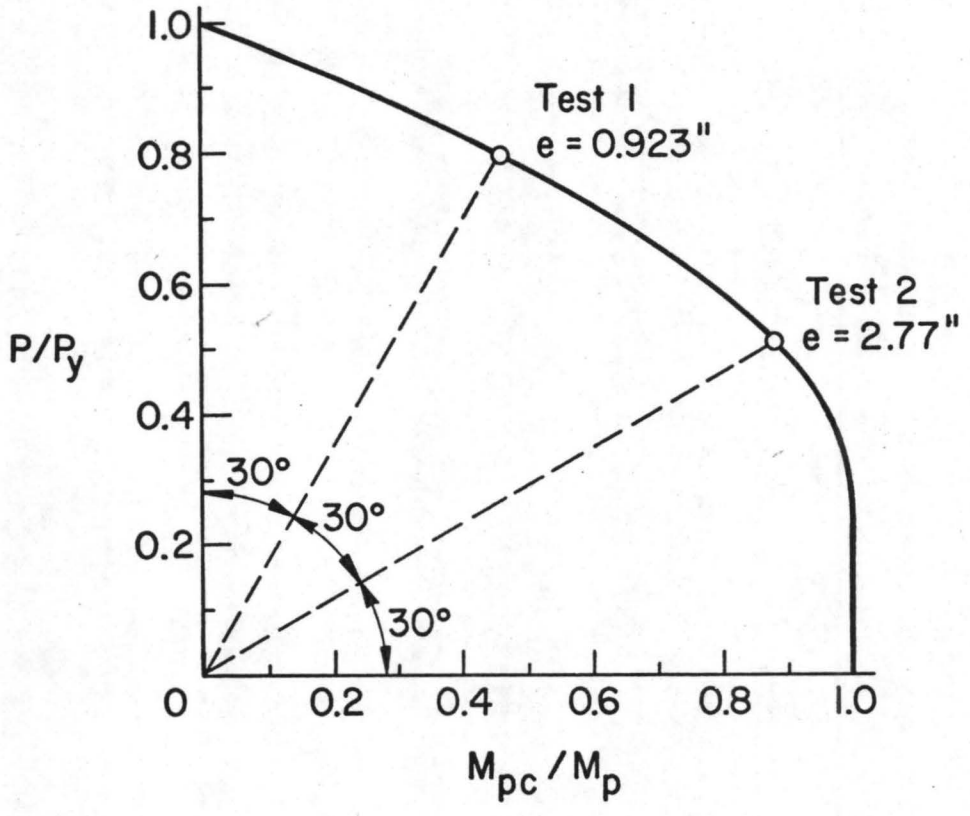

FIG. 4 DETERMINATION OF TEST ECCENTRICITIES

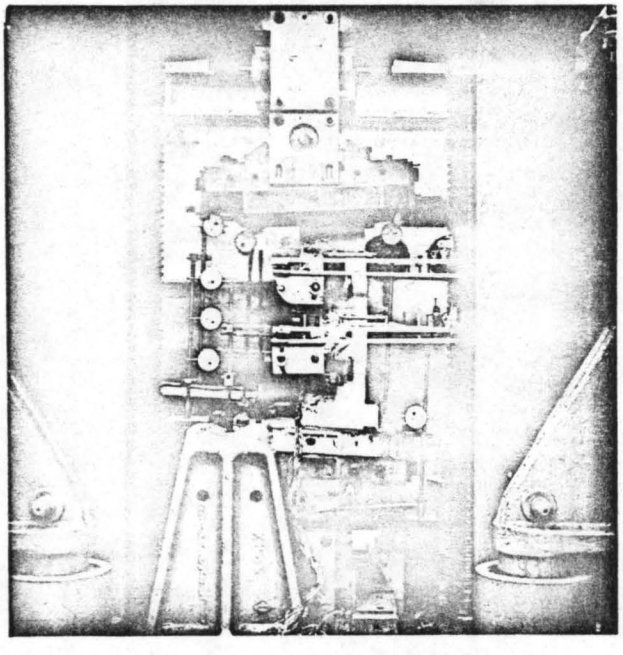

FIG. 5 TEST SETUP

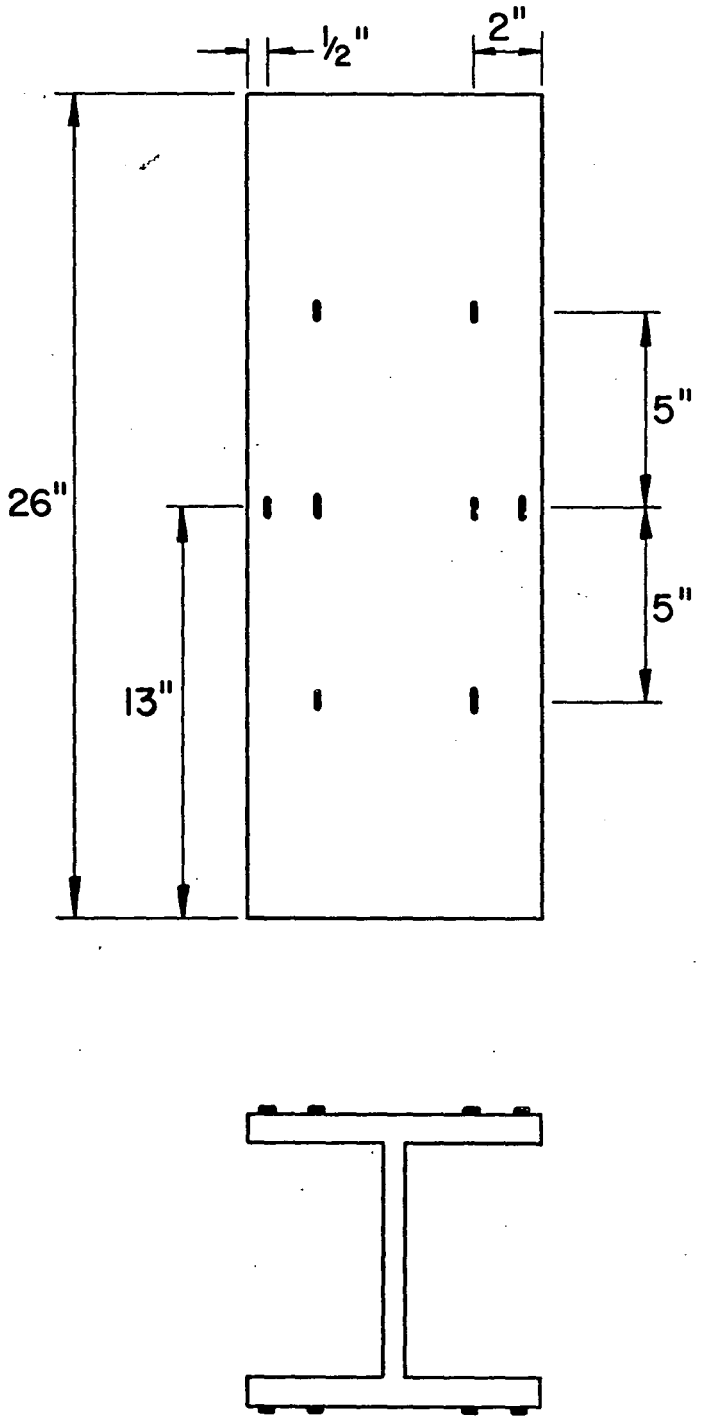

FIG. 6 POSITIONS OF STRAIN GAGES ON SPECIMEN

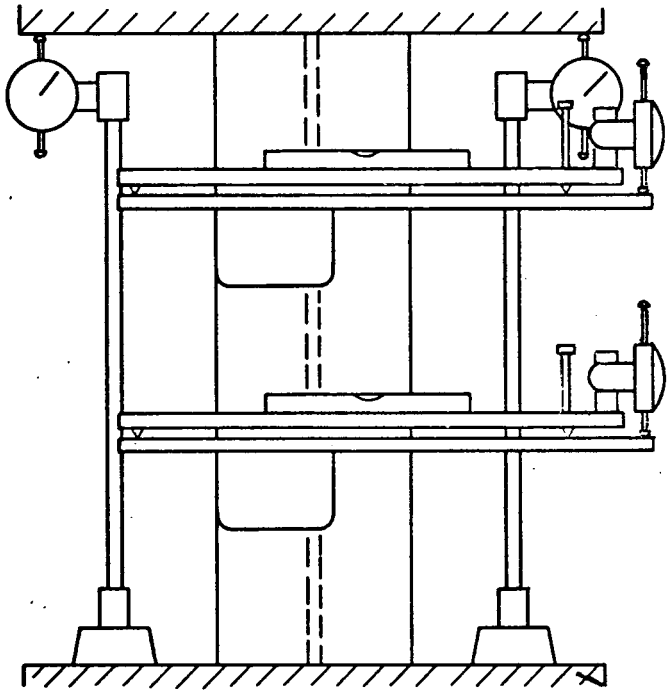

FIG. 7 POSITIONS OF ROTATION GAGES

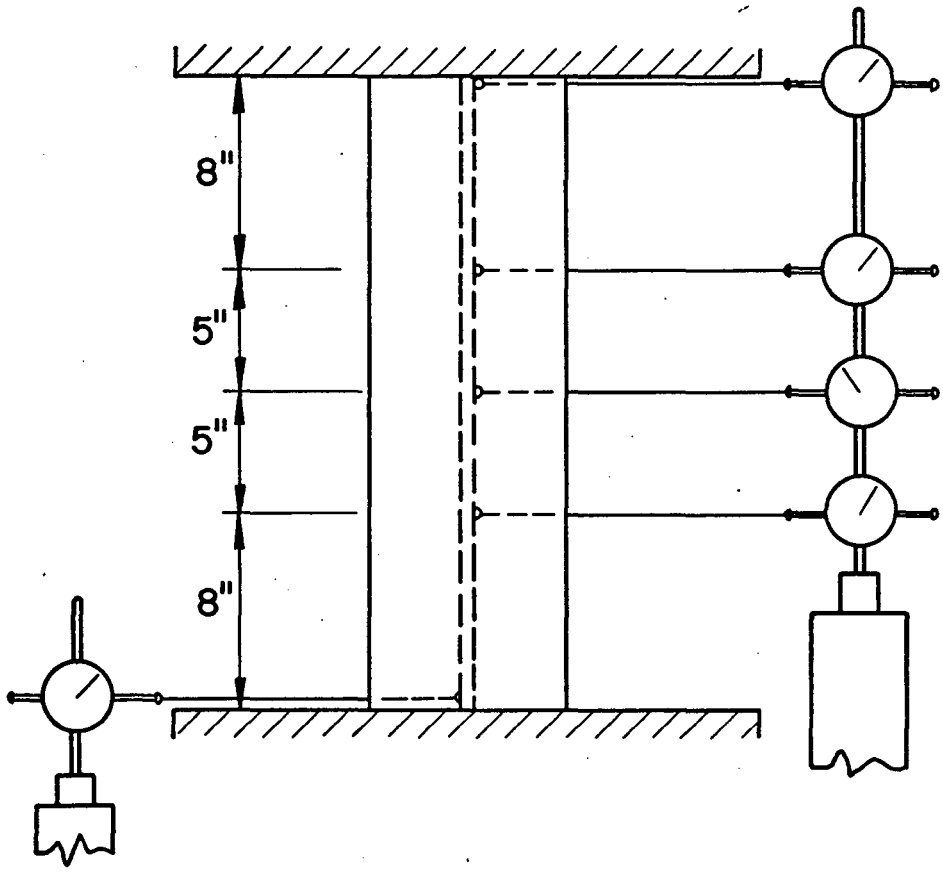

FIG. 8 POSITIONS OF DEFLECTION GAGES

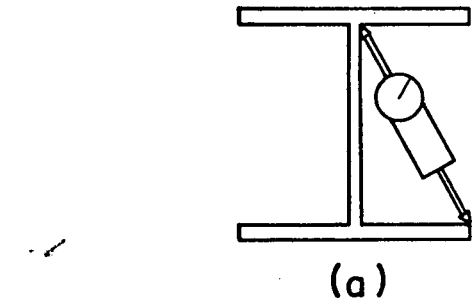

(a)

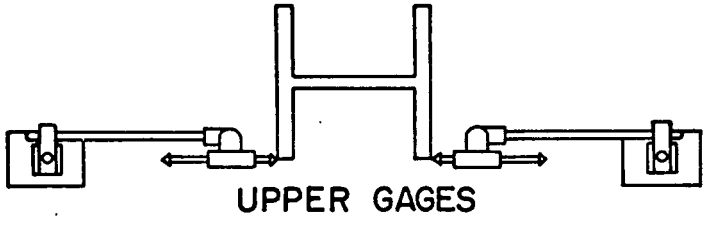

UPPER GAGES

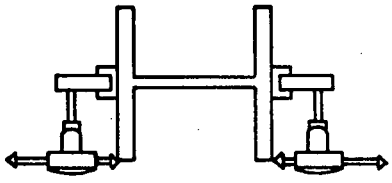

MIDDLE GAGES

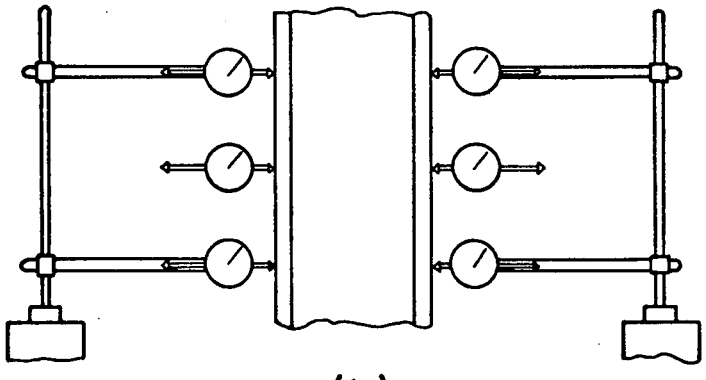

(b)

FIG. 9 TWO METHODS OF MEASURING FLANGE BUCKLING

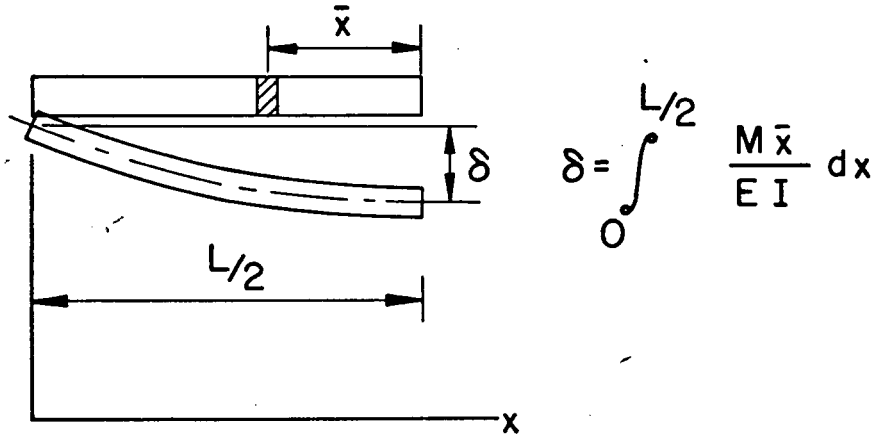

FIG. 10 DETERMINATION OF SLOPE OF LOAD-DEFLECTION RELATION

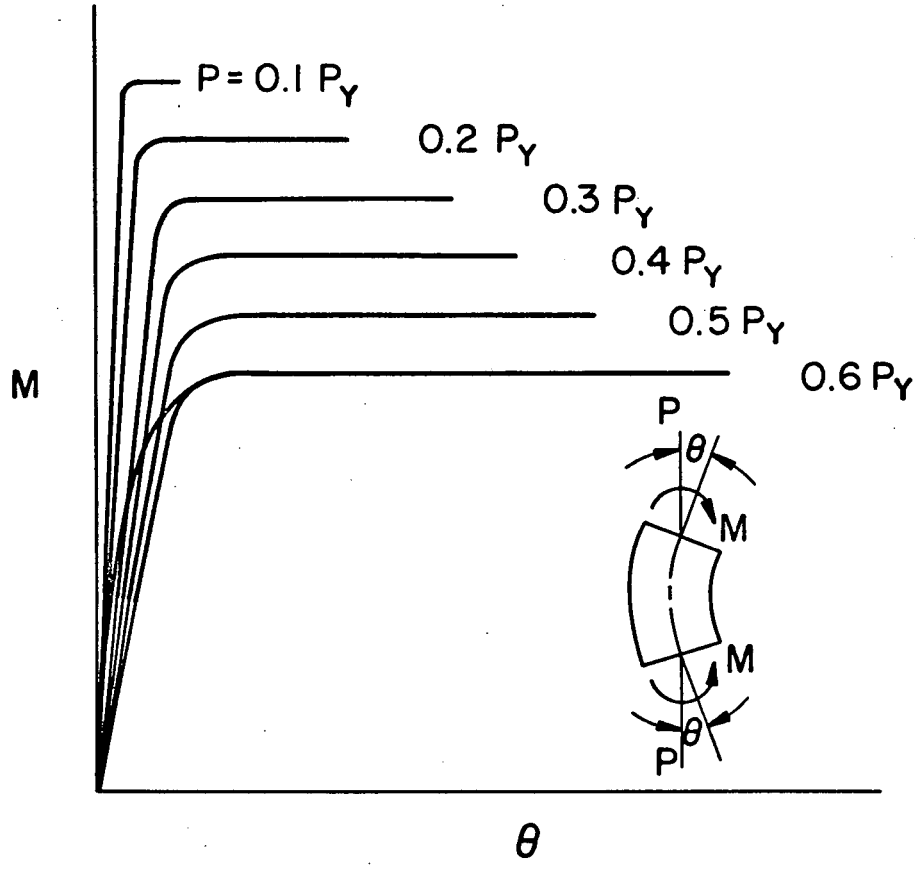

FIG. 11 DETERMINATION OF THEORETICAL MOMENT-ROTATION RELATION

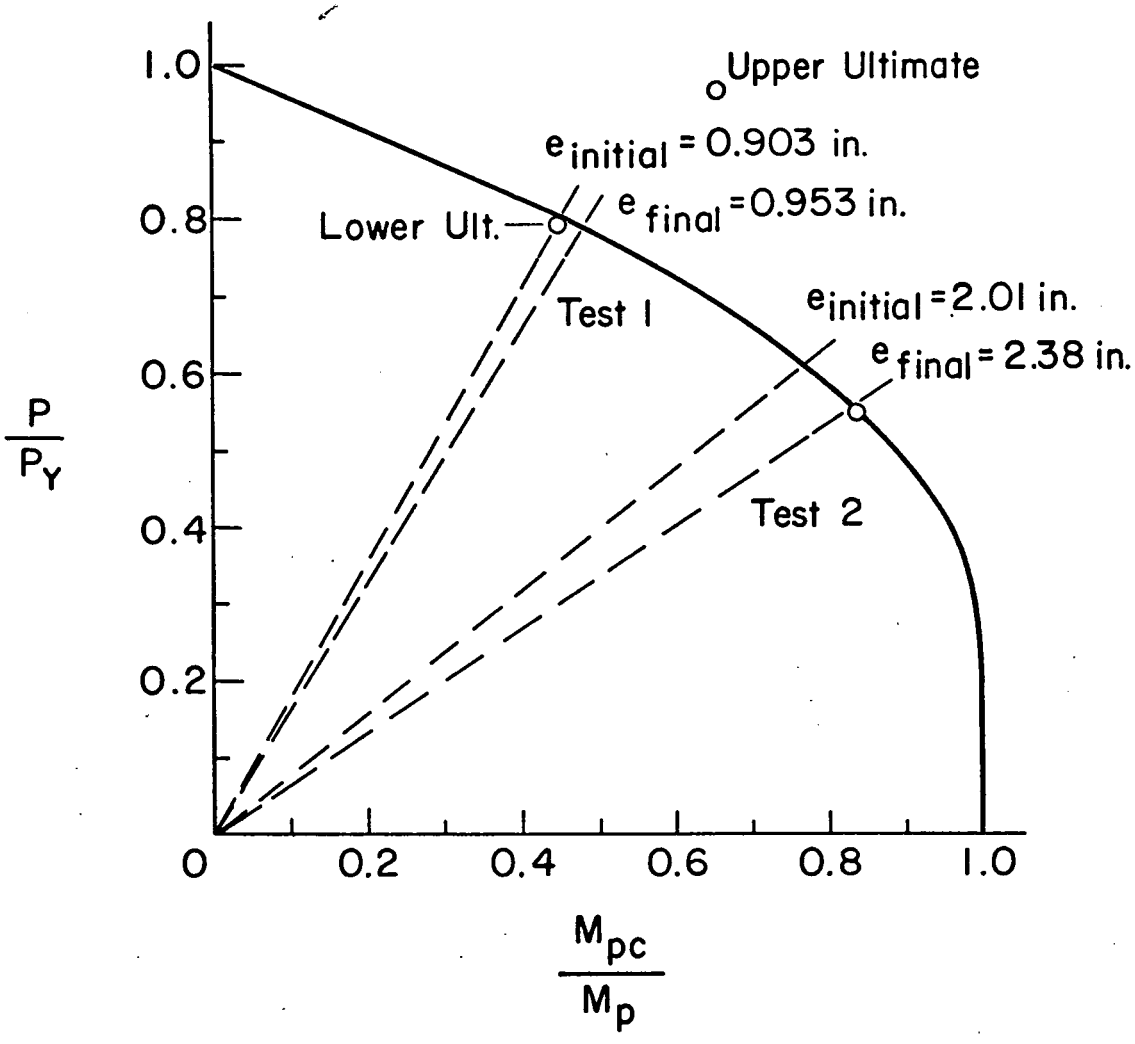

FIG. 12 INTERACTION RELATION

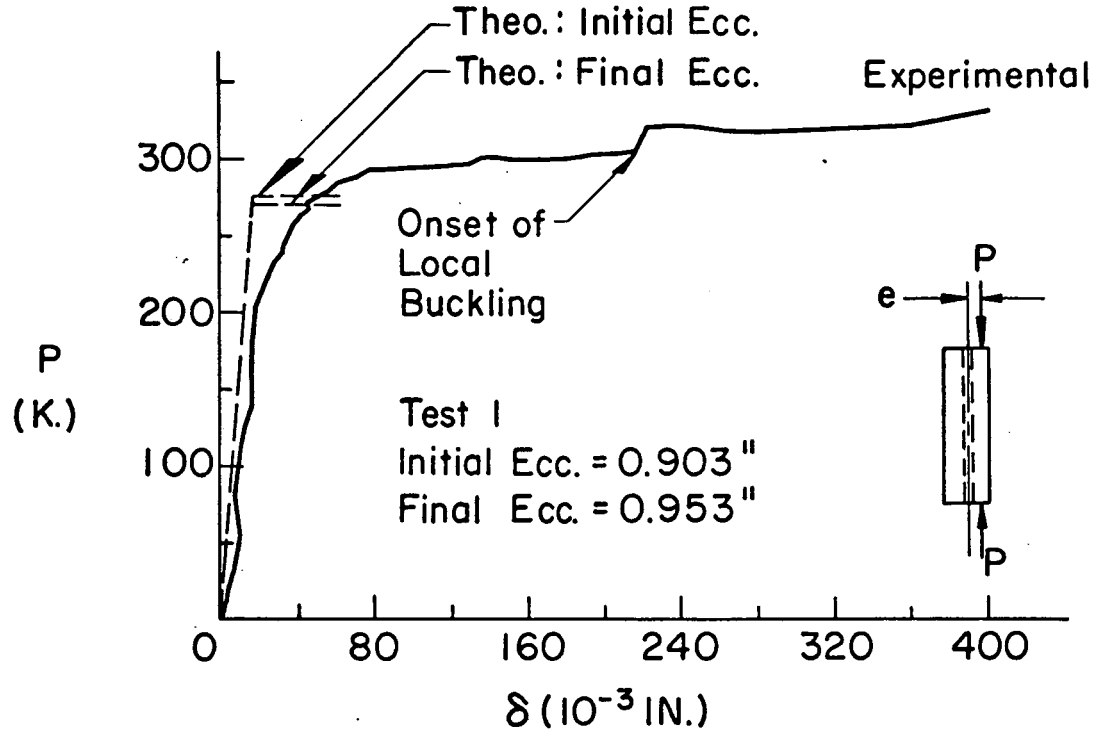

FIG. 13a LOAD-DEFLECTION RELATION - TEST NO. 1

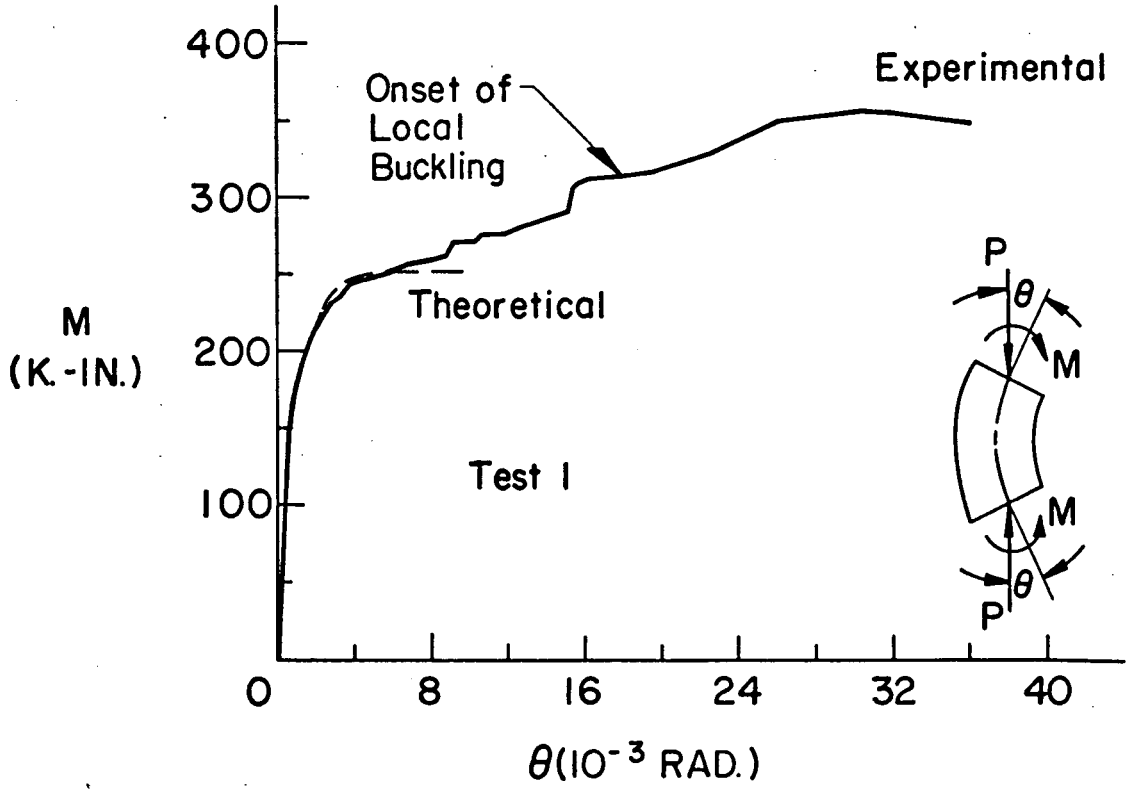

FIG. 13b MOMENT-ROTATION RELATION - TEST NO. 1

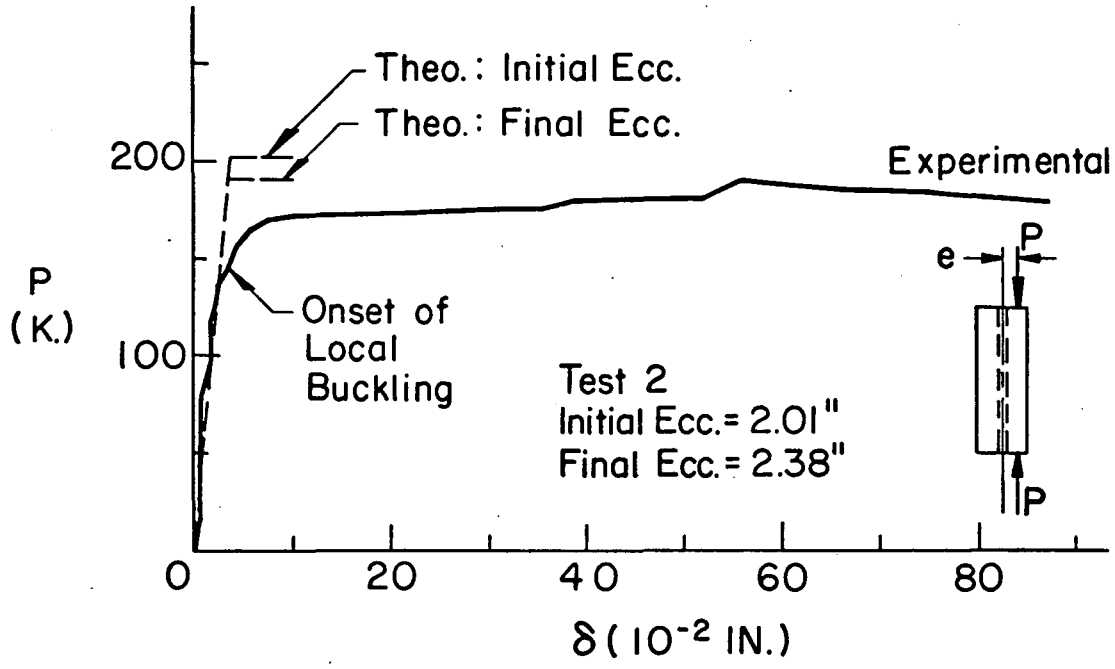

FIG. 14a LOAD-DEFLECTION RELATION - TEST NO. 2

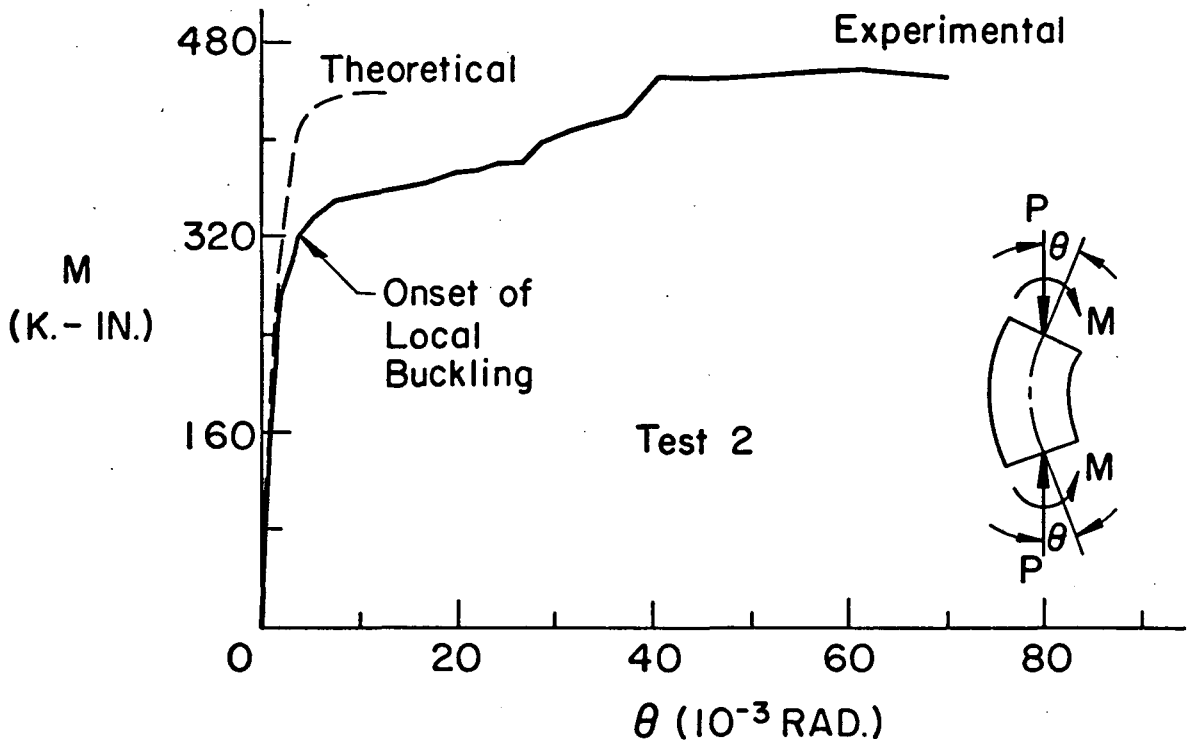

FIG. 14b MOMENT-ROTATION RELATION - TEST NO. 2

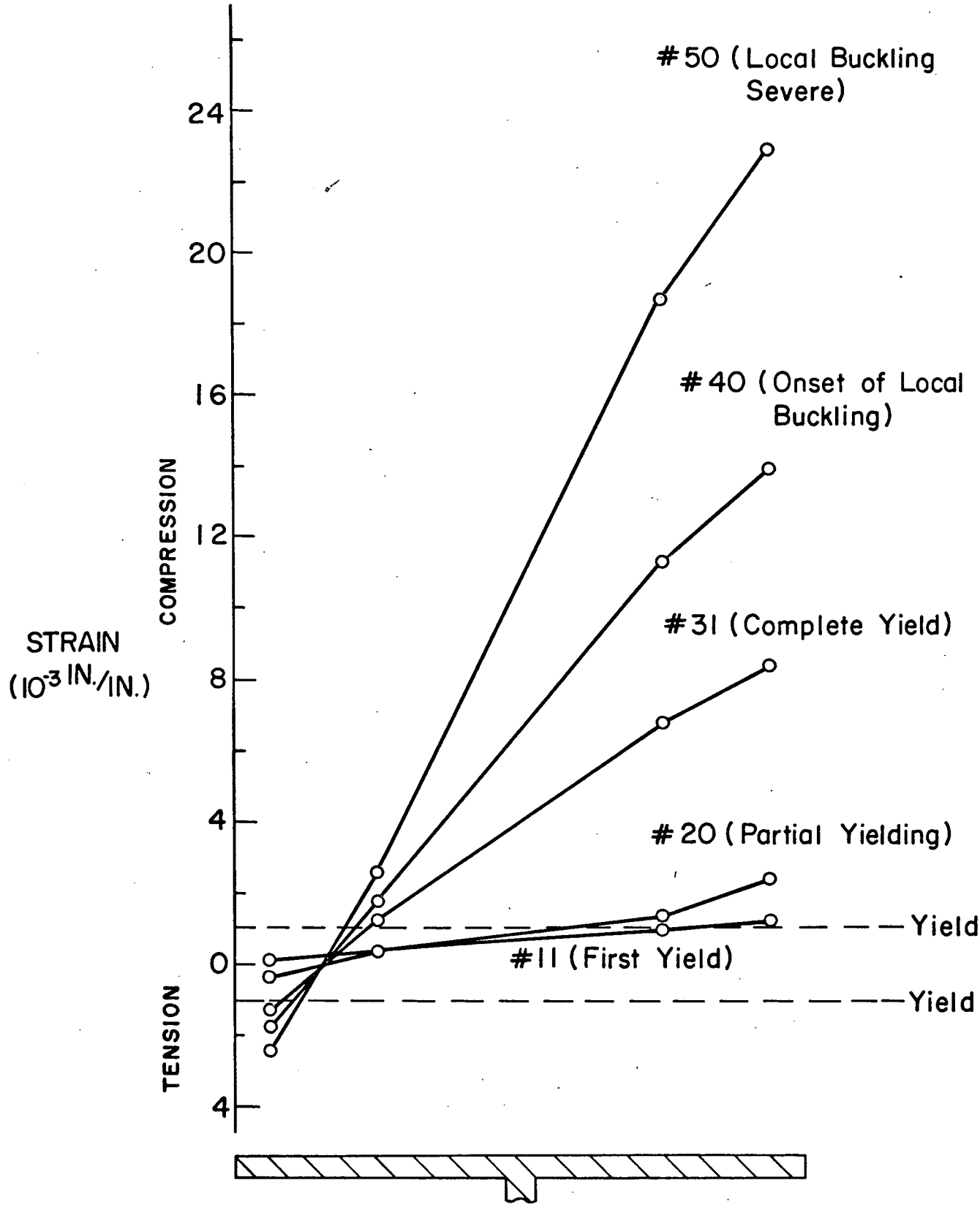

FIG. 15 STRAIN DISTRIBUTION ACROSS WEST-FLANGE AT MIDHEIGHT TEST NO. 1

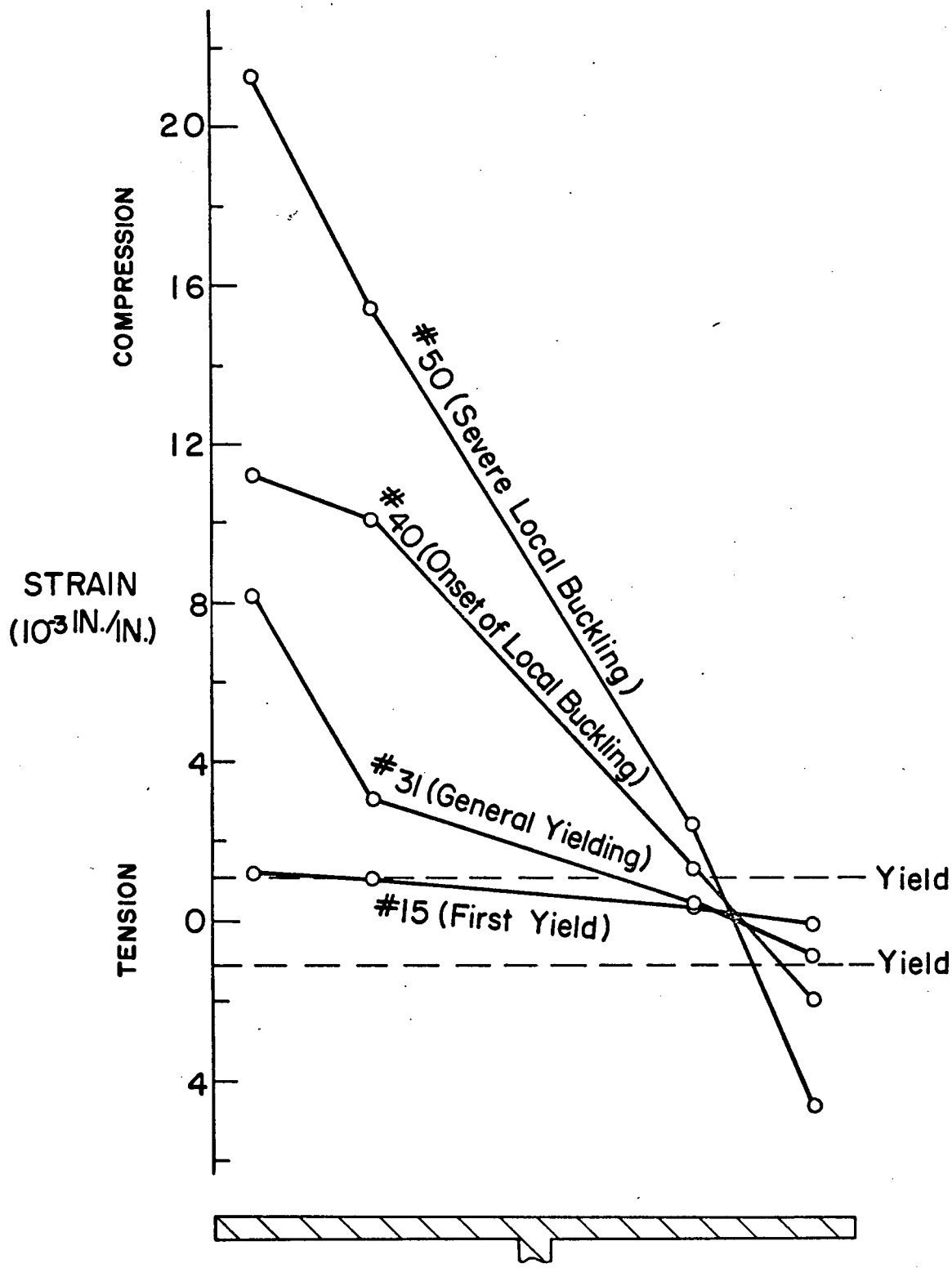

FIG. 16 STRAIN DISTRIBUTION ACROSS EAST FLANGE AT MIDHEIGHT TEST NO. 1

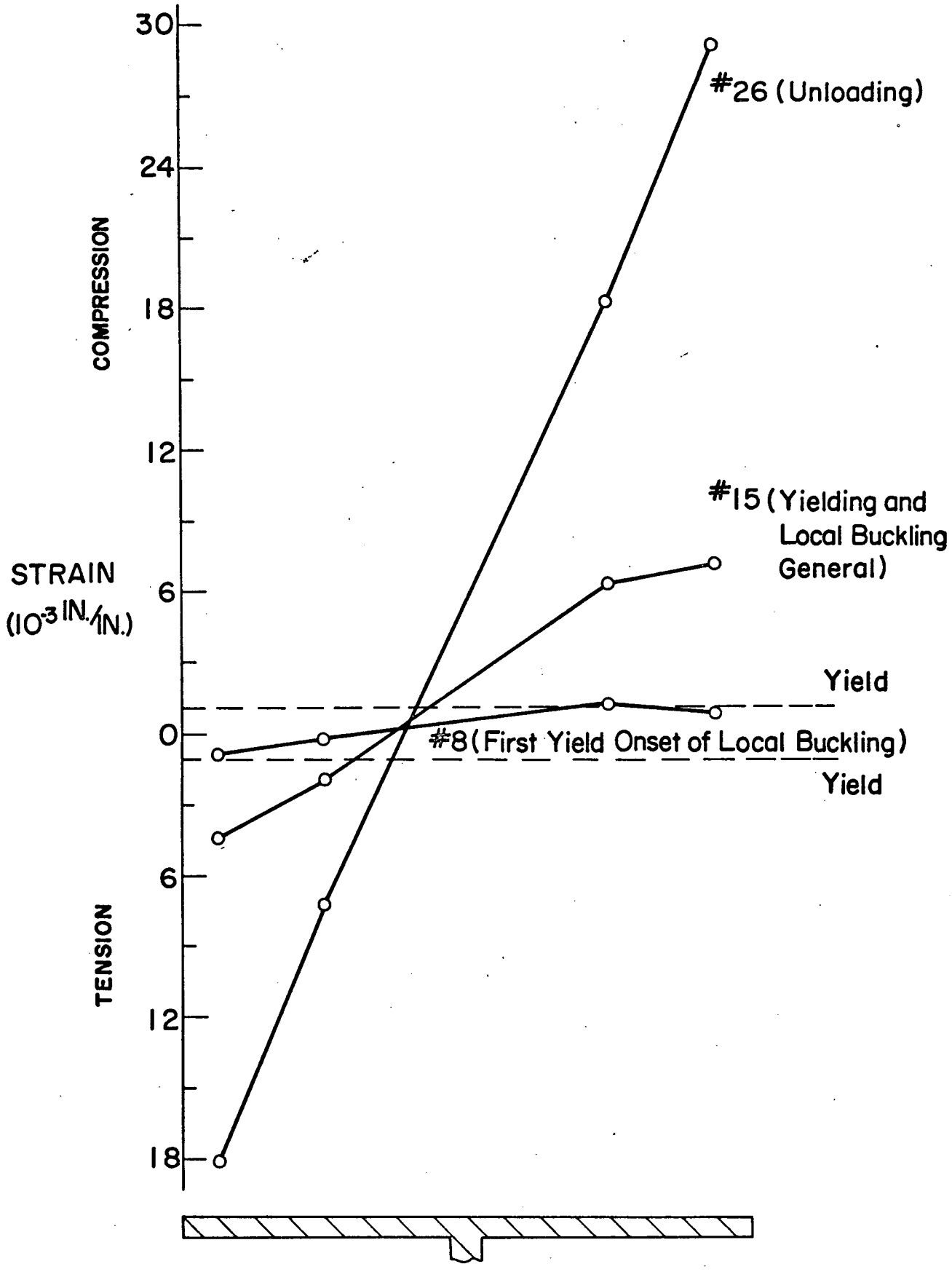

FIG. 17 STRAIN DISTRIBUTION ACROSS WEST FLANGE AT MIDHEIGHT TEST NO. 2

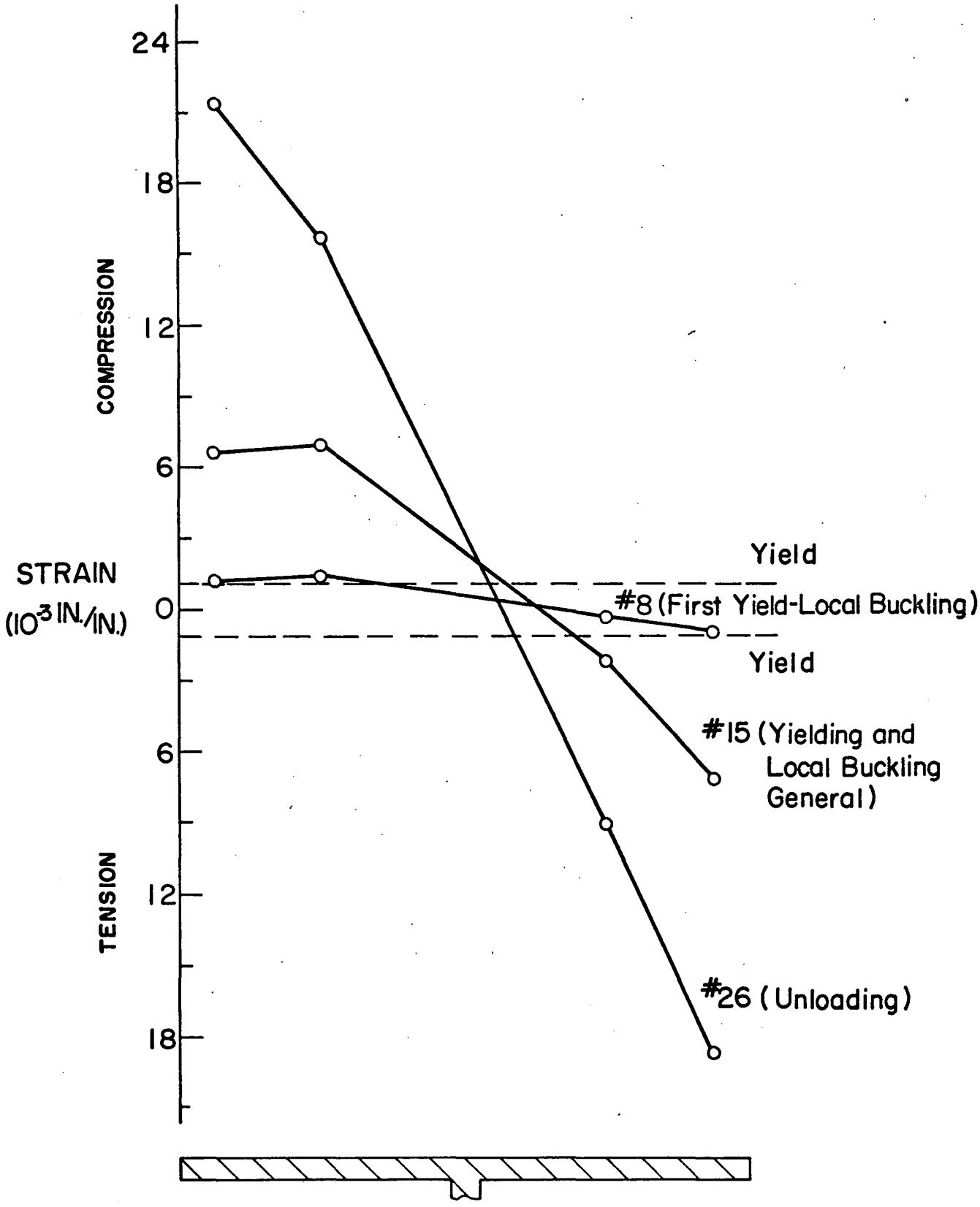

FIG. 18 STRAIN DISTRIBUTION ACROSS EAST FLANGE AT MIDHEIGHT-TEST NO. 2

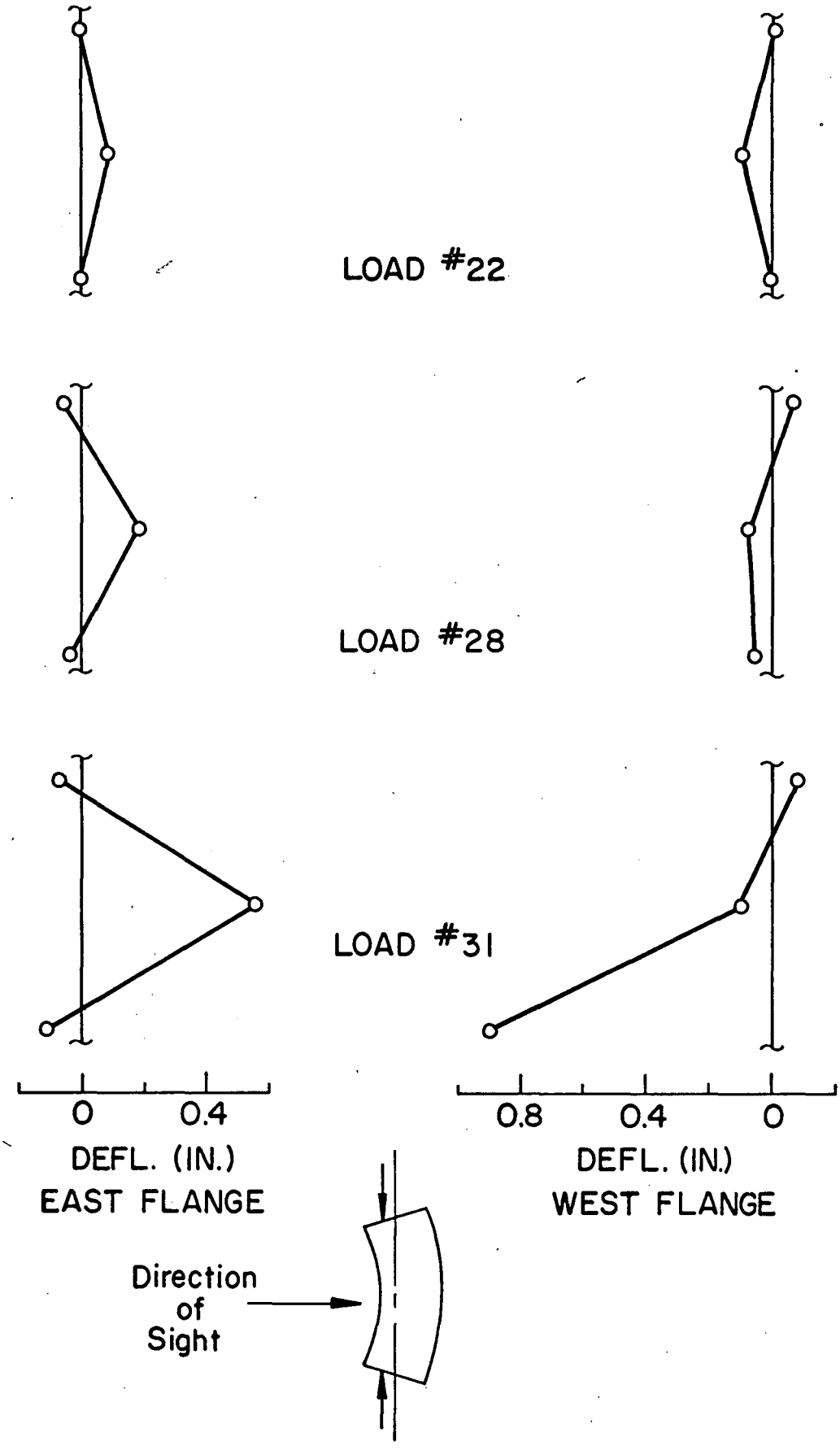

FIG. 19 FLANGE DEFORMATIONS-TEST NO. 2

8. REFERENCES

1. Ojalvo, M. and Levi, V.
   COLUMNS IN PLANAR AND CONTINUOUS STRUCTURES, Proc. ASCE, Vol. 89, No. ST1, p. 1, 1963.

2. Galambos, T. V. and Fukumoto, Y.
   INELASTIC LATERAL-TORSIONAL BUCKLING OF BEAM-COLUMNS, Proc. ASCE, Vol. 92, No. ST2, p. 41, 1966.

3. Galambos, T. V., Adams, P. F. and Fukumoto, Y.
   FURTHER STUDIES ON THE LATERAL-TORSIONAL BUCKLING STRENGTH OF STEEL BEAM-COLUMNS, Welding Research Council Bulletin No. 115, 1966.

4. Lu, L. W.
   COLUMNS, Lecture No. 4, Conference on "Plastic Design of Multi-Story Frames," Lehigh University, 1965.

5. Galambos, T. V.
   COMBINED BENDING AND COMPRESSION, Chapter 11, STRUCTURAL STEEL DESIGN, edited by L. Tall, Ronald Press, 1964.

6. Lay, M. G.
   FLANGE LOCAL BUCKLING IN WIDE-FLANGE SHAPES, Proc. ASCE, Vol. 91, No. ST6, p. 95, 1965.

7. WRC-ASCE Committee
   COMMENTARY ON PLASTIC DESIGN IN STEEL, ASCE Manual 41, Chapter 7, 1961.

8. Lay, M. G. and Gimsing, N.
   EXPERIMENTAL STUDIES ON THE MOMENT-THRUST-CURVATURE RELATIONSHIP, Welding Journal, Vol. 44, No. 2, February 1965.

9. Lim, L. C., Scheid, R. A. and Lu, L. W.
   COMPUTER PROGRAM FOR M-P-$\emptyset$, CDC, AND M-θ RELATIONSHIPS OF WIDE-FLANGE BEAM-COLUMNS BENT ABOUT STRONG OR WEAK AXIS, Fritz Laboratory Report No. 329.4, November 1970.

10. Galambos, T. V.
    STRUCTURAL MEMBERS AND FRAMES, Chapter 5, Prentice-Hall, 1968.